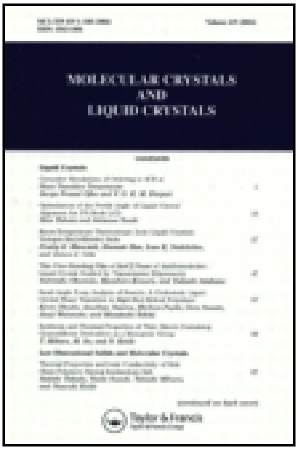

Molecular Crystals and Liquid Crystals

Publication details, including instructions for authors and subscription information:
http://www.tandfonline.com/loi/gmcl20

Synthesis and Spectral Properties of Tris(Terphenylylpyridine)Iridium and Tris(Tritylphenylpyridine)Iridium Complexes as Novel Electrophosphorescent Materials

Chie Honda [a], Kazuo Takimiya [a], Tetsuo Otsubo [a] & Yoshio Aso [b]

[a] Department of Applied Chemistry, Graduate School of Engineering, Hiroshima University, Higashi-Hiroshima, Japan

[b] The Institute of Scientific and Industrial Research, Osaka University, Ibaraki, Japan

Version of record first published: 31 Jan 2007

To cite this article: Chie Honda, Kazuo Takimiya, Tetsuo Otsubo & Yoshio Aso (2006): Synthesis and Spectral Properties of Tris(Terphenylylpyridine)Iridium and Tris(Tritylphenylpyridine)Iridium Complexes as Novel Electrophosphorescent Materials, Molecular Crystals and Liquid Crystals, 455:1, 373-379

To link to this article: http://dx.doi.org/10.1080/15421400600698964

Mol. Cryst. Liq. Cryst., Vol. 455, pp. 373–379, 2006
Copyright © Taylor & Francis Group, LLC
ISSN: 1542-1406 print/1563-5287 online
DOI: 10.1080/15421400600698964

Synthesis and Spectral Properties of Tris(Terphenylylpyridine)Iridium and Tris(Tritylphenylpyridine)Iridium Complexes as Novel Electrophosphorescent Materials

Chie Honda
Kazuo Takimiya
Tetsuo Otsubo
Department of Applied Chemistry, Graduate School of Engineering,
Hiroshima University, Higashi-Hiroshima, Japan

Yoshio Aso
The Institute of Scientific and Industrial Research, Osaka University,
Ibaraki, Japan

*Three novel iridium complexes (***2a–c***) have been synthesized as structural modifications of a promising electrophosphorescent material, Ir(ppy)$_3$ (***1***). The dichloromethane solutions of these complexes like* **1** *showed a broad metal-to-ligand charge transfer band at around 380 nm in the absorption spectra and at around 520 nm in the emission spectra. In contrast to that of Ir(ppy)$_3$, the film phases of* **2a–c** *show remarkable emission owing to the prevention of aggregation quenching due to their bulky ligands. Organic electroluminescence devices using* **2a–c** *emitted green light.*

Keywords: electrophosphorescent material; iridium complex; organic electroluminescence device; photoluminescence

INTRODUCTION

Recent utilization of highly efficient electrophosphorescent materials made a breakthrough in organic electroluminescence (EL) device performance [1]. One of the most promising electrophosphorescent materials is *fac* tris(2-phenylpyridine) iridium (**1**), Ir(ppy)$_3$ [2], and

Address correspondence to Tetsuo Otsubo, Department of Applied Chemistry, Graduate School of Engineering, Hiroshima University, Higashi-Hiroshima 739-8527, Japan. E-mail: otsubo@hiroshima-u.ac.jp

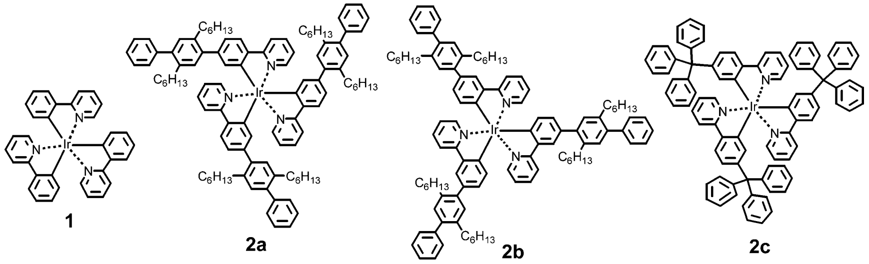

CHART 1

the development of highly efficient EL materials by its chemical modifications has attracted current attention [3]. Here we would like to report three novel iridium complexes (**2a–c**), which involve terphenylylpyridine or (tritylphenyl)pyridine ligands (Chart 1).

RESULTS AND DISCUSSION

The three compounds **2a–c** were synthesized via the dinuclear complexes **4a–c** by tris-cyclometallation of iridium trichloride trihydrate with the corresponding terphenylylpyridine or (tritylphenyl)pyridine compounds (**3a–c**) according to the protocol shown in Scheme 1 [4]. The key compounds **3a–c** were derived from known compounds **5** [5], **8** [6], and **12** [7], respectively, by utilizing conventional Suzuki coupling or Stille coupling, as shown in Scheme 2. All new compounds were characterized by spectroscopic and elemental analyses [8]. The proton NMR spectra of **2a,b** display twelve kinds of distinct aromatic proton resonances, indicating that the three ligands surrounding the iridium atom are magnetically equivalent and therefore, they have facial C_3 symmetrical structures. No signals assignable to the meridional isomers with C_1 symmetrical structures were observed.

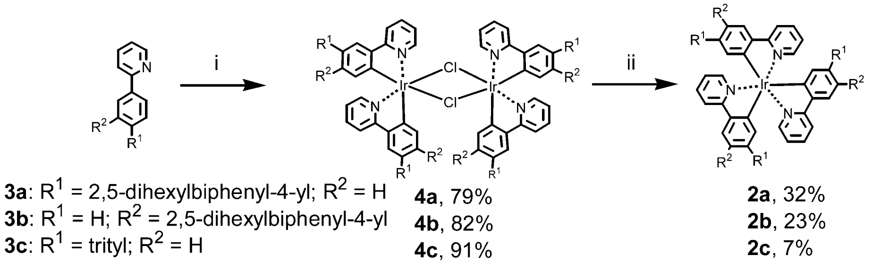

SCHEME 1 Reagents and conditions: i) $IrCl_3 \cdot 3H_2O$, 3:1 diglyme–water, reflux, 18 h; ii) 3.5 equiv **3a–c** CF_3SO_3Ag, ethylene glycol, 110–140 °C, 24 h.

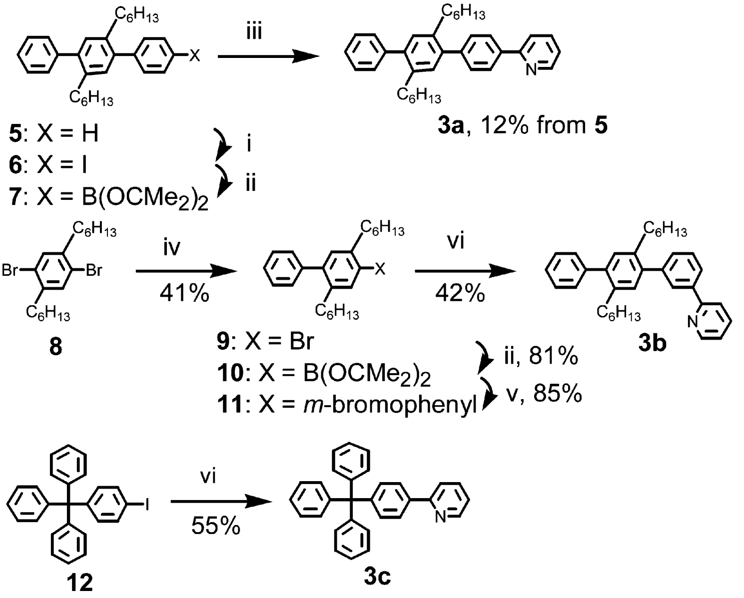

SCHEME 2 Reagents and conditions: i) I_2, H_5IO_6, 10:2:0.3 AcOH–H_2O–H_2SO_4, reflux, 24 h; ii) *n*-BuLi, −78 °C, 0.5 h then 2-isopropoxy-4,4-5,5-tetramethyl-1,3,2-dioxaborolane, rt, 3 h; iii) 2-bromopyridine, cat Pd(PPh_3)$_4$, K_3PO_4, DMF, 120 °C, 11 h; iv) phenylboronic acid, cat Pd(PPh_3)$_4$, 1:1 toluene–NaOH aq, reflux, 44 h; v) *m*-bromoiodobenzene, 1:1 toluene–NaOH aq, reflux, 60 h; vi) 2-tributylstannylpyridine, cat Pd(PPh_3)$_4$, toluene, reflux, 14 h.

Ten kinds of aromatic proton resonances observed in the NMR spectrum of **2c** also supported the existence of only the facial isomer.

Figure 1 shows the electronic absorption spectra of **1** and **2a–c** measured in dichloromethane, and Table 1 summarizes their specific peak positions together with those measured in the film phase. All absorption spectra have essentially the same features: intense ligand-localized transition (LT) bands in the short wavelength region (240–310 nm) and a broad metal-to-ligand charge-transfer (MLCT) band in the long wavelength region (around 380 nm). These absorption bands tend to be red-shifted in the film phase, presumably being ascribable to molecular aggregation. However, it is worthy noticing that the red shifts for **2a–c** are smaller than those for Ir(ppy)$_3$ (**1**), and the MLCT band of **2b** is rather blue-shifted. Evidently the bulky ligands tend to prevent aggregation in the film phase.

As shown in Figure 2, the emission spectra of Ir(ppy)$_3$(**1**) and **2a–c** exhibit a broad phosphorescence band at around 520 nm due to MLCT

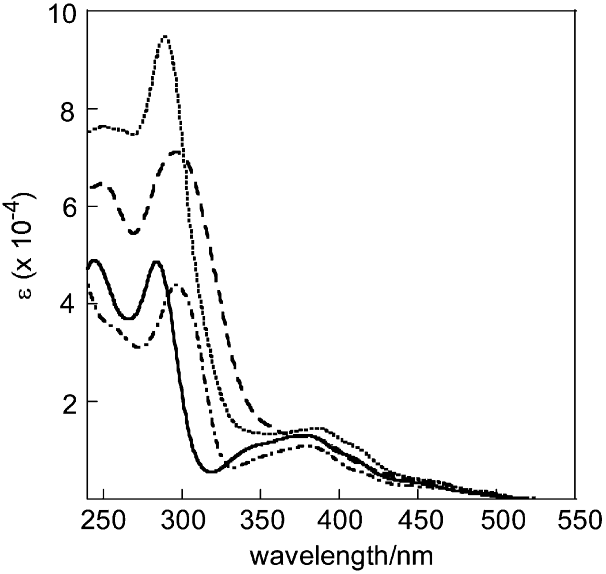

FIGURE 1 UV-Vis absorption spectra of **1** (solid line), **2a** (broken line), **2b** (dot line), and **2c** (dot-dash line) in dichloromethane.

transition. On comparison to that of **1**, the photoluminescence intensities of **2a–c** are considerably weakened and the photoluminescence maxima are a little red-shifted. Evidently the extension of the ligand π-systems function so as to reduce the MLCT emission. In the film phase, the photoluminescence of **1** becomes very weak and red-shifted because of molecular aggregation. On the other hand, the film phases

TABLE 1 Electronic Absorption and Emission Data of **1** and **2a–c**

Compd		$\lambda_{\max}$ (abs)/nm LT	$\lambda_{\max}$ (abs)/nm MLCT	$\lambda_{\max}$ (emis)/nm
1	Solution[a]	244, 284	377	515
	Film	246, 296	387	527 (very weak)
2a	Solution[a]	250, 296	388	524
	Film	251, 298	389	526
2b	Solution[a]	250, 289	386	525
	Film	289	380	520
2c	Solution[a]	257, 296	379	525
	Film	262, 305	387	527

[a] Measured in dichloromethane.

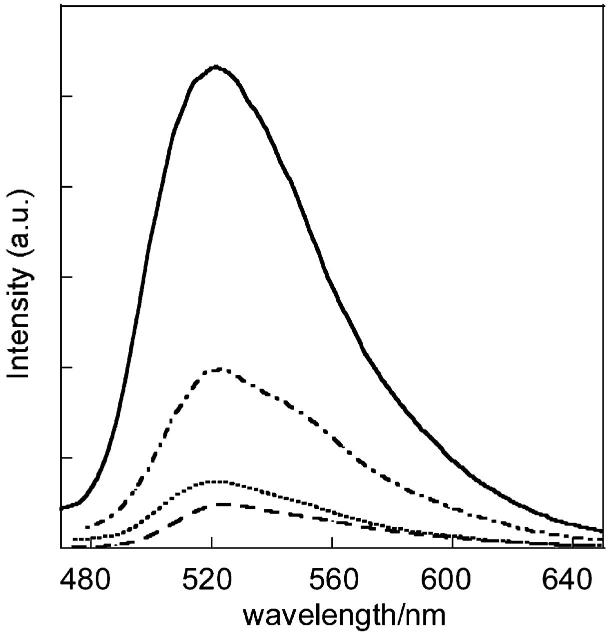

FIGURE 2 Emission spectra of **1** (solid line), **2a** (broken line), **2b** (dot line), and **2c** (dot-dash line) upon excitation at MLCT band in dichloromethane, where the absorbances of all samples are kept constant.

of **2a–c** still show remarkable photoluminescence. Little shifts of the emission bands in film relative to those in solution also indicate no or less aggregation in the films of **2a–c**. In particular, it is notable that the MLCT photoluminescence band of **2b** is blue-shifted, similarly to the case for the MLCT absorption band. This spectral difference between the regioisomers **2a** and **2b** may be related to both different sterical and electronic effects depending on substitution sites in the 2-phenylpyridine ligands of Ir(ppy)$_3$.

Thanks to the bulky ligands, all three iridium complexes (**2a–c**) are highly soluble in common solvents, being superior in thin film processability. Thus they have a potential as promising electrophosphorescent materials for organic electroluminescence (EL) devices. A preliminary experiment demonstrated that all EL devices based on **2a–c** emitted green light, whose spectra are almost identical to their photoluminescence spectra. Specifically, the device with the configuration, ITO/5% **2a**-CBP (100 nm)/BCP (30 nm)/LiF (0.7 nm)/Al [9], demonstrated maximum luminance 15 cd/m^2 (6.8 V) and power efficiency 0.12 lm/W.

REFERENCES

[1] (a) Baldo, M. A., O'Brien, D. F., You, Y., Shoustikov, A., Sibley, S., Thompson, M. E., & Forrest, S. R. (1998). *Nature*, *395*, 151.

(b) O'Brien, D. F., Baldo, M. A., Thompson, M. E., & Forrest, S. R. (1999). *Appl. Phys. Lett.*, *74*, 442.

[2] Baldo, M. A., Lamansky, S., Burrows, P. E., Thompson, M. E., & Forrest, S. R. (1999). *Appl. Phys. Lett.*, *75*, 4.

[3] (a) Ostrowski, J. C., Robinson, M. R., Heeger, A. J., & Bazan, G. C. (2002). *Chem. Commun.*, 784.

(b) Lo, S.-C., Male, N. A. H., Markham, J. P. J., Magennis, S. W., Burn, P. L., Salata, O. V., & Samuel, I. D. W. (2002). *Adv. Mater.*, *14*, 975.

(c) Lo, S.-C., Namdas, E. B., Burn, P. L., & Samuel, I. D. W. (2003). *Macromolecules*, *36*, 9721.

(d) Markham, J. P. J., Samuel, I. D. W., Lo, S.-C., Burn, P. L., Weiter, M., & Bässler, H. (2004). *J. Appl. Phys.*, *95*, 438.

(e) Frampton, M. J., Namdas, E. B., Lo, S.-C., Burn, P. L., & Samuel, I. D. W. (2004). *J. Mater. Chem.*, *14*, 2881.

[4] Colombo, M. G., Brunold, T. C., Riedener, T., Güdel, H. U., Förtsch, M., & Bürgi, H.-B. (1994). *Inorg. Chem.*, *33*, 545.

[5] Galda, P. & Rehahn, M. (1996). *Synthesis*, 614.

[6] Rehahn, M., Schlüter, A.-D., & Feast, W. J. (1988). *Synthesis*, *386*.

[7] Li, Q., Rukavishnikov, A. V., Petukhov, P. A., Zaikova, T. O., & Keana, J. F. W. (2002). *Org. Lett.*, *4*, 3631.

[8] Selected data of **2a**: yellow powder; mp 74–75°C; ^{1}H NMR (400 MHz, $CDCl_3$) δ 7.91 (br d, $J = 8.3$ Hz, 3 H), 7.68 (d, $J = 8.0$ Hz, 3 H), 7.61 (br td, $J = 8.3$, 1.5 Hz, 3 H), 7.57 (br dd, $J = 5.1$, 1.5 Hz, 3 H), 7.35–7.25 (A_2B_2C m, 15 H), 7.08 (d, $J = 1.8$ Hz, 3 H), 7.01 (s, 3 H), 6.89 (s, 3 H), 6.88–6.85 (m, 3 H), 6.85 (dd, $J = 8.0$, 1.8 Hz, 3 H), 2.50–2.35 (m, 6 H), 2.35–2.20, (m, 6 H), 1.50–1.30 (m, 6 H), 1.25–1.10 (m, 36 H), 0.95–0.85 (m, 6 H), 0.77 (t, $J = 6.6$ Hz, 9 H), 0.72 (t, $J = 7.4$ Hz, 9 H); MS (MALDI-TOF) m/z 1616.11 (M^+, calcd 1615.91). **2b**: yellow powder; mp 107–108°C; ^{1}H NMR δ 7.90 (br d, $J = 8.3$ Hz, 3 H), 7.66 (d, $J = 1.8$ Hz, 3 H), 7.65 (br dd, $J = 5.1$, 1.2 Hz, 3 H), 7.62 (br td, $J = 8.3$, 1.2 Hz, 3 H), 7.44–7.32 (A_2B_2C m, 15 H), 7.19 (s, 3 H), 7.10 (s, 3 H), 7.01 (d, $J = 7.9$ Hz, 3 H), 6.94 (br dd, $J = 8.3$, 5.1 Hz, 3 H), 6.90 (dd, $J = 7.9$, 1.7 Hz, 3 H), 2.65 (m, 12 H), 1.52–1.44 (m, 12 H), 1.24–1.08 (m, 36 H), 0.78 (t, $J = 6.8$ Hz, 9 H), 0.74 (t, $J = 7.1$ Hz, 9 H); MS m/z 1615.94 (M^+, calcd 1616.49). **2c**: yellow powder; mp > 300°C; ^{1}H NMR δ 7.79 (br d, $J = 7.9$ Hz, 3 H), 7.51 (br td, $J = 7.9$, 1.2 Hz, 3 H), 7.45 (br dd, $J = 4.9$, 1.2 Hz, 3 H), 7.16 (d, $J = 8.5$ Hz, 3 H), 7.05–6.98 (m, 9H), 6.95–6.65 (m, 36H), 6.67 (br dd, $J = 7.9$, 4.9 Hz, 3 H), 6.59 (br s, 3 H), 6.43 (d, $J = 8.5$ Hz, 3 H); MS m/z 1381.97 (M^+, calcd 1381.49). **3a**: pale yellow oil; ^{1}H NMR δ 8.73 (ddd, $J = 4.9$, 2.2, 1.1 Hz, 1 H), 8.06 (d, $J = 8.1$ Hz, 2 H), 7.81 (ddd, $J = 7.8$, 2.2, 1.1 Hz, 1 H), 7.76 (td, $J = 7.8$, 1.7 Hz, 1 H), 7.49 (d, $J = 8.1$ Hz, 2 H), 7.45–7.38 (m, 5 H), 7.25 (ddd, $J = 7.8$, 4.9, 1.1 Hz, 1 H), 7.17 (s, 1 H), 7.15 (s, 1 H), 2.62–2.55 (m, 4 H), 1.55–1.40 (m, 4 H), 1.30–1.10 (m, 12 H), 0.81 (t, $J = 6.8$ Hz, 3 H), 0.80 (t, $J = 6.8$ Hz, 3 H); MS m/z 475.97 (M^+, calcd 475.32). **3b**: yellow oil; ^{1}H NMR δ 8.71 (ddd, $J = 4.8$, 1.4, 1.1 Hz, 1 H), 8.02 (dt, $J = 7.8$, 1.7 Hz, 1 H), 7.98 (t, $J = 1.7$ Hz, 1 H), 7.79–7.73 (m, 2 H), 7.54 (t, $J = 7.8$ Hz, Hz, 1 H), 7.45–7.30 (m, 6 H), 7.25 (ddd, $J = 7.8$, 4.9, 1.1 Hz, 1 H), 7.19 (s, 1 H), 7.14 (s, 1 H), 2.59 (t, $J = 7.7$ Hz, 2 H), 2.57 (t, $J = 7.8$ Hz, 2 H), 1.56–1.44 (m, 4 H), 1.25–1.10 (m, 12 H), 0.81 (t, $J = 6.9$ Hz, 3 H), 0.77 (t, $J = 7.0$ Hz, 3 H); MS (EI) m/z 475 (M^+). **3c**: colorless needles; mp 232–233°C; ^{1}H NMR δ 8.66 (ddd, $J = 4.9$, 1.7, 1.2 Hz, 1 H),

7.86 (d, $J = 8.6$ Hz, 2 H), 7.73 (td, $J = 8.0$, 1.7 Hz, 1 H), 7.69 (dt, $J = 8.0$, 1.2 Hz, 1 H), 7.34 (d, $J = 8.6$ Hz, 2 H), 7.27–7.18 (m, 16H); MS (EI) m/z 397 (M^+). **4a**: yellow powder; mp 124–126°C; ^{1}H NMR δ 9.32 (dd, $J = 5.6$, 1.4 Hz, 4 H), 7.87 (dd, $J = 8.0$, 1.5 Hz, 4 H), 7.76 (td, $J = 8.0$, 1.4 Hz, 4 H), 7.52 (d, $J = 8.0$ Hz, 4 H), 7.40–7.25 (m, 20 H), 6.94 (s, 4 H), 6.88 (s, 4 H), 6.78 (dd, $J = 8.0$, 1.5 Hz, 4 H), 6.71 (ddd, $J = 8.0$, 5.6, 1.4 Hz, 4 H), 6.03 (d, $J = 1.5$ Hz, 4 H), 2.44 (t, $J = 7.9$ Hz, 8 H), 2.24–2.34 (m, 8 H), 1.45–1.00 (m, 64 H), 0.81 (t, $J = 6.9$ Hz, 12 H), 0.75 (t, $J = 7.3$ Hz, 12 H); MS m/z 1176.08 (M^{2+}, calcd 1176.56). **4b**: yellow powder; mp 210–212°C; ^{1}H NMR δ 9.34 (dd, $J = 5.9$, 1.5 Hz, 4 H), 7.91, (dd, $J = 8.0$, 1.5 Hz, 4 H), 7.78 (td, $J = 8.0$, 1.5 Hz, 4 H), 7.53 (d, $J = 1.8$ Hz, 4 H), 7.45–7.30 (m, 20 H), 7.08 (s, 4 H), 7.06 (s, 4 H), 6.85 (ddd, $J = 8.0$, 5.9, 1.5 Hz, 4 H), 6.65 (dd, $J = 8.1$, 1.8 Hz, 4 H), 6.10 (d, $J = 8.1$ Hz, 4 H), 2.52 (t, $J = 8.8$ Hz, 8 H), 2.50, (t, $J = 9.0$ Hz, 8 H), 1.51–1.15 (m, 64 H), 0.78 (t, $J = 6.8$ Hz, 12 H), 0.74 (t, $J = 7.1$ Hz, 12 H); MS m/z 1175.26 (M^{2+}, calcd 1176.56). **4c**: yellow powder; mp > 300°C; ^{1}H NMR δ 8.96 (dd, $J = 5.8$, 1.4 Hz, 4 H), 7.47 (dd, $J = 8.0$, 1.2 Hz, 4 H), 7.31 (td, $J = 8.0$, 1.4 Hz, 4 H), 7.23 (d, $J = 8.3$ Hz, 4 H), 7.05–6.95 (m, 36 H), 6.85–6.80 (m, 24 H), 6.57 (dd, $J = 8.3$, 1.7 Hz, 4 H), 6.25 (ddd, $J = 8.0$, 5.8, 1.4 Hz, 4 H), 5.51 (d, $J = 1.7$ Hz, 4 H); MS m/z 1020.19 (M^{2+}, calcd 1020.26).

[9] CBP: 4,4′-*N,N*′-dicarbazole-biphenyl; BCP: 2,9-dimethyl-4,7-diphenyl-1,10- phenanthroline. The 5% **2a**-CBP layer was fabricated by spin coating from dichloromethane solution.